Polymer Journal (2015) 47, 71–76

www.nature.com/pj

ORIGINAL ARTICLE

Aggregation behavior in water of amphiphilic diblock copolymers bearing biocompatible phosphorylcholine and cholesteryl groups

Sayaka Ohno[1], Shoto Hasegawa[1], Huihua Liu[2], Kazuhiko Ishihara[3] and Shin-ichi Yusa[1]

Poly(2-(methacryloyloxy)ethyl phosphorylcholine)-*block*-poly(cholesteryl 6-methacryloyloxyhexanoate) ($PMPC_{82}$-*b*-$PChM_n$) copolymers with different PChM block lengths were prepared via reversible addition–fragmentation chain transfer controlled/living radical polymerization using a PMPC-based macro-chain transfer agent. The subscript number and n (= 3 and 6) refer to the degree of polymerization of the PMPC and PChM blocks, respectively. $PMPC_{82}$-*b*-$PChM_n$ cannot dissolve in water directly due to the strong hydrophobic nature of the PChM block. To prepare the aqueous solution, the diblock copolymer was dissolved in an organic solvent and then dialyzed against pure water. These diblock copolymers formed spherical and rod-like micelles in water, depending on the composition of cholesteryl (Chol) group in the polymer. The prepared aggregates were characterized using static light scattering, dynamic light scattering, transmission electron microscopy and fluorescence probe techniques. The characterization results suggest that the morphology of the polymer aggregates can be controlled from spherical to rod-like micelles by increasing the number of Chol groups in the polymer.
Polymer Journal (2015) **47,** 71–76; doi:10.1038/pj.2014.92; published online 5 November 2014

INTRODUCTION

Self-assembled nanometer-sized aggregates from polymers in solution have been widely investigated recently. The aggregates can be formed via various intermolecular interactions such as hydrophobic, electrostatic, hydrogen bonding and van der Waals interactions.[1–3] Our studies focused on the nanometer-sized aggregates formed via hydrophobic interactions in aqueous solution. Amphiphilic block copolymers can form various types of aggregates through hydrophobic interactions in water once the critical aggregation concentration (CAC) is exceeded.[4] Structures of the formed aggregates strongly depend on the balance of the molecular weights of the hydrophobic and hydrophilic parts in the polymer. It has been reported in the literature that the structure of the formed aggregates changed from spherical to rod-like micelles and to lamellae when the ratio of hydrophobic to hydrophilic part in the polymer was increased.[5] For example, a hydrophobic cholesteryl (Chol) group has a planar and rigid steroid backbone. When Chol groups are introduced onto a flexible alkyl chain, the Chol groups show a liquid crystalline nature.[6] Furthermore, pendant Chol groups in amphiphilic polymers preferably align with lamellae structure in water.[7] Therefore, an amphiphilic polymer containing Chol groups as a hydrophobic unit forms aggregates of various shape, rather than simply spherical micelles, depending on the molecular weighing of the hydrophobic Chol groups.[8,9] Boissé *et al.*[10] have reported that amphiphilic diblock copolymers composed of hydrophilic poly(*N*,*N*-diethylacrylamido) and hydrophobic Chol group-containing blocks showed fiber structures in water. An ellipsoidal vesicle morphology was observed from amphiphilic diblock copolymers composed of hydrophilic poly (ethylene glycol) (PEG) and hydrophobic Chol group-containing blocks in a work by Lia *et al.*[11] Venkataraman *et al.*[12] have reported that amphiphilic diblock copolymers composed of hydrophilic PEG and hydrophobic polycarbonate with pendant Chol groups formed aggregates exhibiting various shapes in water depending on the degree of polymerization (DP) of the hydrophobic block. Specifically, disk-like micelles and stacked-disk morphology are observed from the amphiphilic diblock copolymers when the DP of the hydrophobic block is 4 and 11, respectively.

2-(methacryloyloxy)ethyl phosphorylcholine (MPC) has become a hot research topic due to the unique characteristic of its hydrophilic phosphorylcholine group possessing the same chemical structure as the hydrophilic part of the phospholipids that form cell membranes.[13] Hydrophilic MPC monomers can be used to copolymerize various types of functional vinyl monomers, with excellent biocompatibility and antithrombogenicity. More importantly, properties and functions for the MPC-containing polymer can be precisely controlled by adjusting the comonomers. Various types of homopolymers and copolymers containing MPC were prepared via atom transfer radical polymerization in water or methanol.[14–16] For example, Xu *et al.*[17]

[1]Department of Materials Science and Chemistry, Graduate School of Engineering, University of Hyogo, Hyogo, Japan; [2]School of Health Sciences, Federation University Australia, Mount Helen, Victoria, Australia and [3]Department of Materials Engineering, The University of Tokyo, Tokyo, Japan
Correspondence: Dr S Yusa, Department of Materials Science and Chemistry, Graduate School of Engineering, University of Hyogo, 2167 Shosha, Himeji, Hyogo 671-2280, Japan.
E-mail: yusa@eng.u-hyogo.ac.jp
Received 11 August 2014; revised 9 September 2014; accepted 10 September 2014; published online 5 November 2014

reported that the hydrophilic poly(2-(methacryloyloxy)ethyl phosphorylcholine) (PMPC) containing a Chol group at the polymer chain end forms spherical micelles in water. However, the remaining transition metal catalyst in PMPC prepared via atom transfer radical polymerization limited its application in the biomedical field because the remaining transition metal catalysts are difficult to be completely removed by column chromatography. Consequently, a new polymerization method, reversible addition-fragmentation chain transfer controlled radical polymerization, is applied in the preparation of PMPC by adding a chain transfer agent (CTA) containing a dithioester group, thereby eliminating the usage of the unwanted transition metal catalyst.

In this study, amphiphilic diblock copolymers ($PMPC_{82}$-*block*-poly(cholesteryl 6-methacryloyloxyhexanoate) ($PChM_n$)) composed of hydrophilic PMPC and hydrophobic PChM blocks were prepared via reversible addition–fragmentation chain transfer controlled radical polymerization (Figure 1). The diblock copolymer aqueous solutions were prepared by a dialysis method because the $PMPC_{82}$-*b*-$PChM_n$ cannot dissolve in water directly due to the hydrophobic PChM block. The hydrophobic/hydrophilic balance was adjusted by changing the composition of Chol groups (n) in $PMPC_{82}$-*b*-$PChM_n$. Effects of the hydrophobic/hydrophilic balance for association behavior of the diblock copolymers in water were studied using dynamic light scattering (DLS), static light scattering (SLS), transmission electron microscopy (TEM) and fluorescence probe techniques.

EXPERIMENTAL PROCEDURE

Materials

ChM was synthesized according to the method reported by Shannon.[18] MPC was synthesized as previously reported and recrystallized from acetonitrile.[13] 4-Cyanopentanoic acid dithiobenzoate (CPD) was synthesized according to the method reported by Mitsukami *et al.*[19] 4,4′-Azobis-(4-cyanopentanoic acid) (V-501, >98%) from Wako Pure Chemical (Osaka, Japan) was used as received. 2,2′-Azobis (2-methylpropionitrile) (AIBN) was purified by recrystallization from methanol. *N*-Phenyl-1-naphthylamine (PNA, >98.0%) was purchased from Tokyo Chemical Industry (Tokyo, Japan). Methanol, ethanol and tetrahydrofuran (THF) were dried by molecular sieves 4 Å and purified by distillation. Water was purified using a Millipore (Billerica, MA, USA) Milli-Q system. Other reagents were used as received.

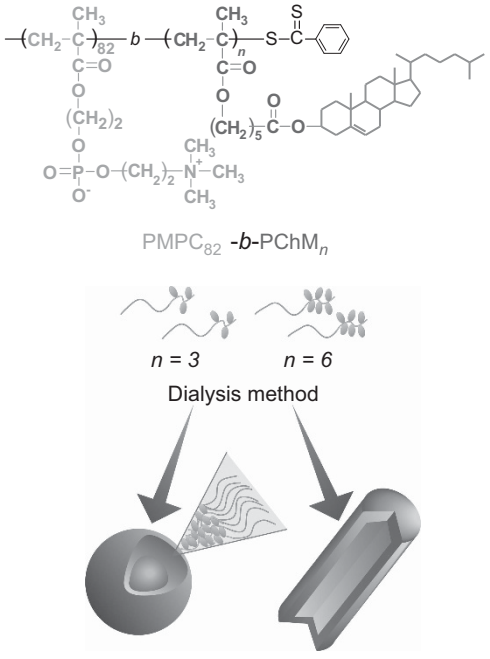

Figure 1 Schematic representation of $PMPC_{82}$-*b*-$PChM_n$ aggregates. A full color version of this figure is available at *Polymer Journal* online.

Preparation of $PMPC_{82}$

MPC (12.0 g, 40.6 mmol) was dissolved in water (9.06 ml). CPD (0.11 g, 0.41 mmol) and V-501 (56.9 mg, 0.20 mmol) were dissolved in methanol (36.3 ml), which was added to the aqueous solution. The solution was deoxygenated by purging with Ar gas for 30 min. Polymerization was carried out at 70 °C for 2 h followed by ^{1}H NMR analysis. The ^{1}H NMR result indicated that the conversion is determined to 97.2%. The reaction mixture was dialyzed against pure water for 2 days and subsequently freeze dried to recover the MPC homopolymer ($PMPC_{82;}$ 11.1 g, 92.4%). Number-average molecular weight (M_n(GPC)) and molecular weight distribution (M_w/M_n) estimated from gel-permeation chromatography (GPC) were 1.75×10^4 and 1.16, respectively. M_n (NMR) and DP were determined from the ^{1}H NMR peak integral intensity ratio of the pendant methine proton at 3.6 p.p.m. and terminal phenyl protons at 7.5–7.9 p.p.m. M_n(NMR) and DP were calculated to be 2.45×10^4 and 82, respectively. The obtained $PMPC_{82}$ was used as a CTA to prepare block copolymers.

Preparation of amphiphilic diblock copolymer ($PMPC_{82}$-*b*-$PChM_n$)

ChM (0.164 g, 0.288 mmol) was dissolved in THF (7.39 ml). $PMPC_{82}$ (1.04 g, 0.0424 mmol, M_n(NMR) = 2.45×10^4, $M_w/M_n = 1.16$) and AIBN (2.70 mg, 0.0164 mmol) were dissolved in ethanol (3.94 ml), which was then added to the THF solution. The solution was deoxygenated by purging with Ar gas for 30 min. Polymerization was carried out at 60 °C for 16 h followed by ^{1}H NMR analysis. After the reaction, ^{1}H NMR analysis indicated that conversion was 72.5%. The reaction mixture was dialyzed against THF for 2 days and against pure water for an additional 2 days. The diblock copolymer ($PMPC_{82}$-*b*-$PChM_3$) was recovered by freeze drying (0.839 g, 69.9%). M_n(NMR) for the diblock copolymer and DP for the PChM block were determined from the ^{1}H NMR peak integral intensity ratio of the methyl protons at 0.7 p.p.m. and pendant methine protons at 3.6 p.p.m. in the PChM and PMPC blocks, respectively. M_n(NMR) and DP were calculated to be 2.59×10^4 and 3, respectively.

$PMPC_{82}$-*b*-$PChM_6$ was prepared via a similar procedure of preparation and purification of $PMPC_{82}$-*b*-$PChM_3$. The conversion was 74.2% as estimated from ^{1}H NMR analysis. M_n(NMR) for $PMPC_{82}$-*b*-$PChM_3$ and DP for the PChM block were calculated to be 2.79×10^4 and 6, respectively.

Measurements

^{1}H NMR spectra were obtained with a Bruker BioSpin (Billerica, MA, USA) DRX-500 spectrometer. GPC measurements were performed using a refractive index detector equipped with a Shodex (Tokyo, Japan) Asahipak GF-1G guard column and 7.0 μm bead size GF-7 M HQ column working at 40 °C under a flow rate of 0.6 ml min^{-1}. A phosphate buffer (pH 9) containing 10 vol% acetonitrile was used as the eluent. The values of M_n(GPC) and M_w/M_n were calibrated with standard sodium poly(styrenesulfonate) samples. SLS and DLS measurements were performed at 25 °C with an Otsuka Electronics Photal (Osaka, Japan) DLS-7000 light scattering spectrometer equipped with an ALV (Langen, Germany) 5000E multi-τ digital time correlator. Sample solutions were filtered with a 0.2-μm pore size membrane filter. A He–Ne laser (10 mW at 632.8 nm) was used as a light source. The weight-average molecular weight (M_w), z-average radius of gyration (R_g) and second virial coefficient (A_2) values were estimated from equation (1):

$$\frac{KC_P}{R_\theta} = \frac{1}{M_w}\left(1 + \frac{1}{3}\langle R_g^2\rangle q^2\right) + 2A_2C_P \quad (1)$$

where R_θ is the Rayleigh ratio; $K = 4\pi^2n^2(dn/dC_p)2/N_A\lambda^4$, with n being the refractive index of the solvent, dn/dC_p the refractive index increment against C_p, C_p the polymer concentration, N_A the Avogadro number and λ the wavelength (= 632.8 nm); $q = (4\pi n/\lambda)\sin(\theta/2)$, with θ being the scattering angle. By measuring R_θ for a set of C_p and θ, values of M_w, R_g and A_2 can be estimated from Zimm plots.[20] Toluene was used for the calibration of the instrument. Values of dn/dC_p were determined with an Otsuka Electronics Photal

DRM-1020 differential refractometer at a wavelength of 632.8 nm. DLS measurements were also performed using a Malvern (Worcestershire, MA, UK) Instruments Zetasizer Nano ZS equipped with a He–Ne laser (4 mW at 633 nm). Data were taken at a 173° scattering angle. In the DLS measurements, inverse Laplace transform analysis was performed using the algorithm REPES [21] to obtain the relaxation time distribution, $\tau A(\tau)$.

$$g^{(1)}(t) = \int \tau A(\tau)\exp(-t/\tau)d\ \ln\tau \qquad (2)$$

where τ is the relaxation time and $g^{(1)}(t)$ is the normalized autocorrelation function. The diffusion coefficient (D) is calculated from $D=\Gamma/q^2$, where Γ is relaxation rate ($\Gamma=\tau^{-1}$). The hydrodynamic radius (R_h) is given by the Stokes–Einstein equation, $R_h=k_BT/(6\pi\eta D)$, where k_B is the Boltzmann constant, T is the absolute temperature and η is the solvent viscosity. TEM measurements were performed with a JEOL (Tokyo, Japan) TEM-1200 electron microscope operated at an accelerating voltage of 200 kV. Samples for TEM were prepared by placing one drop of the aqueous solution on a copper grid coated with thin films of Formvar. Excess water was blotted using filter paper. The samples were stained by sodium phosphotungstate and dried under vacuum for 1 day.

Critical aggregation concentration

Fluorescence spectra were recorded on a Hitachi High-Technologies (Tokyo, Japan) F-2500 fluorescence spectrophotometer. The polymer aqueous solution was mixed with a PNA-saturated aqueous stock solution. The polymer concentration of the mixed aqueous solution was diluted using PNA aqueous solution. The PNA concentration was constant, whereas C_p was diluted. The solutions were excited at 330 nm, and the excitation and emission slit widths were maintained at 20 and 5 nm, respectively.

Preparation of $PMPC_{82}$-*b*-$PChM_n$ aggregates

$PMPC_{82}$-*b*-$PChM_n$ was dissolved in a mixed solution of THF and ethanol (THF/ethanol = 3/7, v/v) at $C_p = 1.0\ g\,l^{-1}$. The solution was transferred to a dialysis bag, which was dialyzed against pure water for 24 h at room temperature. The final C_p of the aqueous solution after dialysis was adjusted to $0.2\ g\,l^{-1}$ by dilution with pure water.

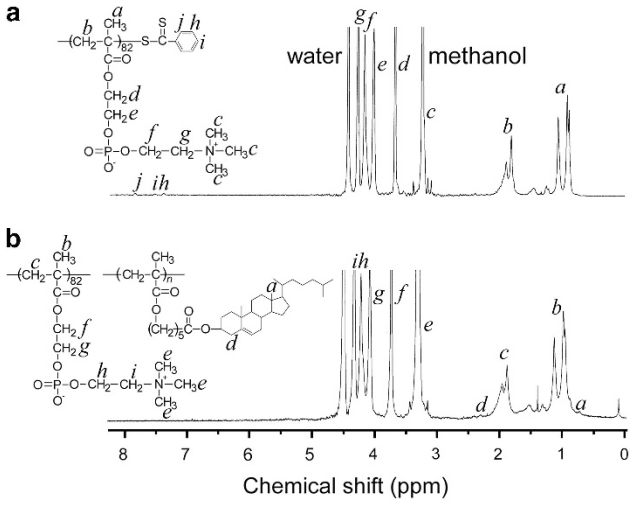

Figure 2 ^{1}H NMR spectra for (**a**) $PMPC_{82}$ and (**b**) $PMPC_{82}$-*b*-$PChM_6$ in methanol-d_4 at 60 °C.

RESULTS AND DISCUSSION

Characterization of $PMPC_{82}$-*b*-$PChM_n$

Figure 2 compares the ^{1}H NMR spectra for $PMPC_{82}$ and $PMPC_{82}$-*b*-$PChM_6$ in methanol-d_4 at 60 °C. The DP and M_n(NMR) for $PMPC_{82}$ are 82 and 2.45×10^4, respectively, and were estimated by comparing the integral intensity area of the terminal phenyl protons at 7.5–7.9 p.p.m. and the pendant methylene protons at 3.6 p.p.m. The DP, M_n(NMR), M_n(GPC) and M_w/M_n values for $PMPC_{82}$ are summarized in Table 1. If the polymerization was assumed to be an ideally living process, the theoretical number-average molecular weight (M_n(theo)) can be calculated from the following equation:

$$M_n(\text{theo}) = \frac{[M]_0}{[CTA]_0}\frac{\chi_m}{100}M_m + M_{CTA} \qquad (3)$$

where $[M]_0$ is the initial monomer concentration, $[CTA]_0$ is the initial CTA concentration, χ_m is the percent conversion of the monomer, M_m is the molecular weight of the monomer and M_{CTA} is the molecular weight of CTA. The M_n(theo) value was found to be near to the M_n(NMR) value for $PMPC_{82}$ and the M_w/M_n for $PMPC_{82}$ was narrow (= 1.16). These observations indicate that the prepared $PMPC_{82}$ possessed a well-controlled structure. The DP values (= *n*) of the PChM block and M_n(NMR) for $PMPC_{82}$-*b*-$PChM_n$ were estimated by comparing integral area intensities of the pendant methyl protons in the PChM block at 0.7 p.p.m. and the pendant methylene protons in the PMPC block at 3.6 p.p.m. The DP values were also estimated by comparing integral area intensities of the PChM block at 0.7 p.p.m. and the terminal phenyl protons at 7.5–7.9 p.p.m. These DP values were the same. These results are summarized in Table 1.

Aggregation of $PMPC_{82}$-*b*-$PChM_n$ in water

The diblock copolymers cannot dissolve in water directly due to the strong hydrophobic nature of the PChM block. To obtain an aqueous solution, the diblock copolymer was dissolved in a mixed organic solvent of THF and ethanol (3/7, v/v) and then dialyzed against pure water to change the organic solvent to an aqueous solution. The diblock copolymers are expected to form the aggregates in the aqueous solution. After dialysis, the C_p was adjusted to be $0.2\ g\,l^{-1}$ by diluting the solution using pure water.

Immediately after preparing the aqueous solution, DLS measurements were performed to measure the R_h values. Figure 3a shows unimodal R_h distributions for $PMPC_{82}$-*b*-$PChM_n$. The R_h values for $PMPC_{82}$-*b*-$PChM_3$ and $PMPC_{82}$-*b*-$PChM_6$ in water were 22.8 and 36.4 nm, respectively (Table 2). It can be read that the value of R_h is directly proportional to the PChM block length. Furthermore, the measured R_h values remained unchanged after 1 week. Figure 3b shows the R_h value as a function of C_p from 0.3 to $0.01\ g\,l^{-1}$.

Table 1 M_n, DP and M_w/M_n of the polymers

Polymer	*DP of MPC*	*DP of ChM*	M_n*(theo)*$\times10^4$	M_n*(NMR)*$\times10^4$	M_n*(GPC)*$\times10^4$	M_w/M_n
$PMPC_{82}$	82	—	2.86	2.45	1.75	1.16
$PMPC_{82}$-*b*-$PChM_3$	82	3	2.73	2.59	—	—
$PMPC_{82}$-*b*-$PChM_6$	82	6	3.04	2.79	—	—

Abbreviations: ChM, cholesteryl 6-methacryloyloxyhexanoate; DP, degree of polymerization; M_n(GPC), number-average molecular weight estimated from gel-permeation chromatography; M_n(NMR), number-average molecular weight estimated from ^{1}H NMR; M_n(theo), number-average molecular weight estimated from Equation 3; MPC, 2-(methacryloyloxy)ethyl phosphorylcholine; M_w/M_n, molecular weight distribution.

0.01 g l^{-1} was chosen as the lower limit as the scattering intensity at $C_p < 0.01$ g l^{-1} was too low to determine the R_h values. It could be read that the R_h values for PMPC$_{82}$-*b*-PChM$_n$ did not change on diluting the C_p from 0.3 to 0.01 g l^{-1}. This observation indicated that the aggregates were stable and do not dissociate above $C_p = 0.01$ g l^{-1}. The relaxation rate (Γ) and square of the magnitude of the scattering vector (q^2) for the aggregates formed from PMPC$_{82}$-*b*-PChM$_n$ are shown in Figure 3c. The Γ–q^2 plots for the diblock copolymers are straight lines passing through the origin, thus indicating that the DLS data correspond to a translational diffusive mode.[22,23]

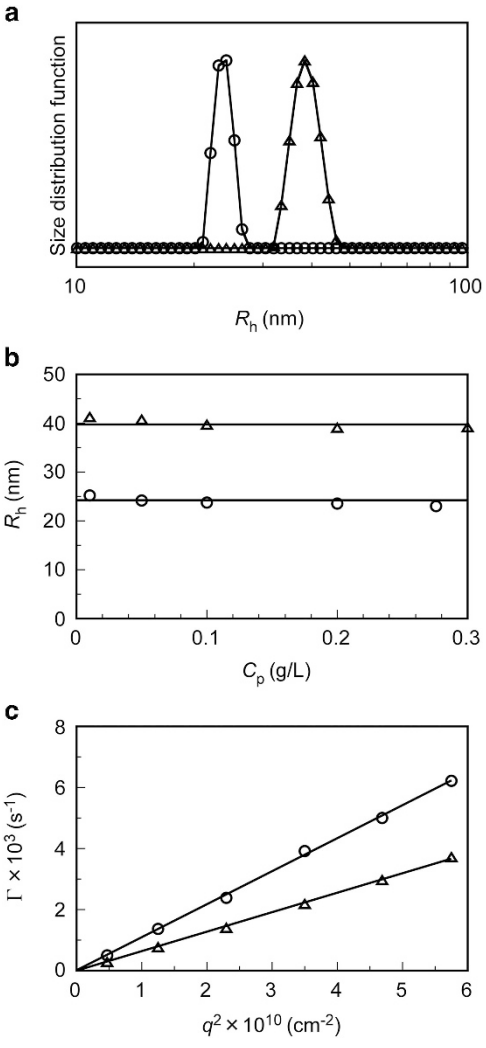

Figure 3 (**a**) Typical examples of hydrodynamic radius (R_h) distributions for aggregates in water at $C_p = 0.2$ g l^{-1}, (**b**) relationship between R_h and C_p for aggregates and (**c**) relationship between the relaxation rate (Γ) and square of the magnitude of the scattering vector (q^2) for aggregates at $C_p = 0.2$ g l^{-1}: PMPC$_{82}$-*b*-PChM$_3$ (○) and PMPC$_{82}$-*b*-PChM$_6$ (Δ).

Characterization of PMPC$_{82}$-*b*-PChM$_n$

SLS measurements were performed in the C_p range of 0.01–0.1 g l^{-1}, where R_h did not change by DLS measurements as determined in the previous section. Figure 4 shows Zimm plots for the diblock copolymers in water. From the chemical structure of the diblock copolymer, it is expected that PMPC$_{82}$-*b*-PChM$_n$ diblock copolymers form core-shell-type aggregates composed of the hydrophobic PChM core and hydrophilic PMPC shell in water. The dn/dC_p values for PMPC$_{82}$-*b*-PChM$_3$ and PMPC$_{82}$-*b*-PChM$_6$ are 0.201 and 0.212 ml g^{-1}, respectively. The SLS data were analyzed using the dn/dC_p values, which are summarized in Table 2. The N_{agg} values were calculated using the ratio between M_w of the aggregate estimated from the SLS and M_w of the unimer estimated from NMR (M_n(NMR)) and GPC (M_w/M_n) data, respectively. The N_{agg} values of the aggregates formed for PMPC$_{82}$-*b*-PChM$_3$ and PMPC$_{82}$-*b*-PChM$_6$ were determined to be 224 and 376, respectively. The apparent M_w, N_{agg} and R_g for the aggregate increased with increasing the chain length of the hydrophobic PChM block as presented in Table 2. Moreover, the A_2 values for PMPC$_{82}$-*b*-PChM$_3$ and PMPC$_{82}$-*b*-PChM$_6$ are 4.09×10^{-4} and 1.61×10^{-4} cm^3 mol g^{-2}, respectively. This finding suggested that the amphiphilic diblock copolymer with long hydrophobic PChM block showed smaller A_2 value, thus indicating that the solubility in water for PMPC$_{82}$-*b*-PChM$_6$ is lower than that for PMPC$_{82}$-*b*-PChM$_3$.[24,25]

The R_g/R_h value is largely related to the shape and polydispersity of aggregates. For example, the R_g/R_h values for rigid hard spheres and spherical shape aggregates are theoretically 0.78 and 1.0, respectively, but these values for random coil and ellipsoidal aggregates are 1.3–1.5. Thread-like and low-density aggregates with high polydispersity index usually exhibit larger R_g/R_h values.[26–28] In the current study, the R_g/R_h value for PMPC$_{82}$-*b*-PChM$_3$ was calculated to be 0.81, which indicated that the aggregate featured as a rigid hard sphere. By contrast, the R_g/R_h value for PMPC$_{82}$-*b*-PChM$_6$ is 1.02. These observations indicated that the aggregate formed from PMPC$_{82}$-*b*-PChM$_6$ is close to spherical shape and the density of the aggregate is lower than that formed from PMPC$_{82}$-*b*-PChM$_3$.

Assuming that the diblock copolymers formed spherical core-shell micelle in water, the core radius (R_c) was calculated using the core volume (V_c) for the aggregate from the equation (4):

$$R_c = \left(\frac{3V_c}{4\pi}\right)^{1/3} = \left(\frac{3}{4\pi N_A}\left(\frac{M_{n,PChM}}{\rho_{PChM}}\right) \times N_{agg}\right)^{1/3} \quad (4)$$

where $M_{n,PChM}$ is the number-average molecular weight of the PChM block, ρ_{PChM} is the density of the PChM block. The cholesterol bulk density (1.05 g cm^{-3}) was used as a ρ_{PChM} value. The R_c values for PMPC$_{82}$-*b*-PChM$_3$ and PMPC$_{82}$-*b*-PChM$_6$ are 5.3 and 9.7 nm, respectively. The density (d) of the aggregate was calculated using the following equation (5):

$$d = \frac{3M_w}{4\pi N_A R_h^3} \quad (5)$$

Table 2 Dynamic and static light scattering data for PMPC$_{82}$-*b*-PChM$_n$ in water

	$M_w \times 10^6$ (g mol^{-1})	R_g (nm)	R_h (nm)	R_g/R_h	N_{agg}	$A_2 \times 10^{-4}$ (cm^3 mol g^{-2})	R_c (nm)	d (g cm^{-3})
PMPC$_{82}$-*b*-PChM$_3$	5.81	18.5	22.8	0.81	224	4.09	5.3	0.19
PMPC$_{82}$-*b*-PChM$_6$	10.5	37.1	36.4	1.02	376	1.61	9.7	0.09

Abbreviations: A_2, the second virial coefficient; d, density of the aggregate estimated from Equation 5; M_w, weight-average molecular weight; N_{agg}, aggregation number for one aggregate; R_c, core radius estimated from Equation 4; R_g, z-average radius of gyration; R_h, hydrodynamic radius.

where M_w is the weight-average molecular weight estimated from SLS measurements. The d values are summarized in Table 2 and will be discussed along with a result of TEM data in the following section.

TEM observations were performed (Figure 5) to investigate the morphologies of the aggregates formed in water. Almost uniform spherical micelles, with an averaged diameter of 25 nm (estimated from TEM data), were observed for $PMPC_{82}$-*b*-$PChM_3$. The average diameter estimated from TEM results were noticed to be smaller than that estimated from DLS measurements. This is probably due to the fact that the diameter estimated from TEM data is a number-average value, whereas the R_h value is an intensity-average value. Furthermore, the samples may shrink during the preparation of the TEM sample. From sample $PMPC_{82}$-*b*-$PChM_6$, TEM observation showed a mixture of morphologies, with some spherical micelles and some rod-like micelles. From TEM data from $PMPC_{82}$-*b*-$PChM_6$ aggregates, the existence number ratio of spherical and rod-like micelles was estimated to be 1:1. The average diameter for the spherical micelles is 25 nm. The minor and major axes for the rod-like micelles are 25 and 50–80 nm, respectively. The formation of the rod-like micelles could be attributed to the increased content of the hydrophobic Chol groups in the diblock copolymer.[29] The rod-like micelles may be formed by intermicellar interactions between the spherical micelles, because $PMPC_{82}$-*b*-$PChM_6$ micelles have less stability and lower dispersity than $PMPC_{82}$-*b*-$PChM_3$ micelles. By contrast, the DLS distribution for $PMPC_{82}$-*b*-$PChM_6$ is unimodal (Figure 3a) because the DLS distribution data for spherical and rod-like micelles cannot be separated as these micelles featured similar sizes. Despite a unimodal DLS distribution, the mixture morphology of spherical and rod-like micelles can be evidenced from the large polydispersity index and small d values. From DLS data, the polydispersity index values for $PMPC_{82}$-*b*-$PChM_3$ and $PMPC_{82}$-*b*-$PChM_6$ are 0.05 and 0.10, respectively. This observation indicated that the aggregates formed from $PMPC_{82}$-*b*-$PChM_6$ were a mixture with different sizes. The d values for $PMPC_{82}$-*b*-$PChM_3$ and $PMPC_{82}$-*b*-$PChM_6$ are 0.19 and 0.09 g cm^{-3}, respectively. The d value for $PMPC_{82}$-*b*-$PChM_6$ suggests that the aggregate formed from $PMPC_{82}$-*b*-$PChM_6$ was a mixture of spherical and low-density rod-like micelles. Furthermore, the low d value for $PMPC_{82}$-*b*-$PChM_6$ may suggest an existence of low-density micelle in the aggregates.

The CAC for $PMPC_{82}$-*b*-$PChM_n$ was measured using a fluorescence probe technique using PNA as a hydrophobic small guest molecule. It is well known that the maximum fluorescence emission wavelength of PNA blue shifts in hydrophobic microenvironment.[30,31] PNA fluorescence probe experiments cannot confirm the core-shell structure that would further determine the CAC values. The PNA fluorescence experiments can only confirm the formation of hydrophobic microdomains, which can incorporate PNA molecules. If a blue shift of the maximum fluorescence wavelength of PNA is observed when increasing the C_p, then the diblock copolymer is assumed to form aggregates incorporating hydrophobic PNA molecules. Figure 6 shows the maximum fluorescence wavelength of PNA

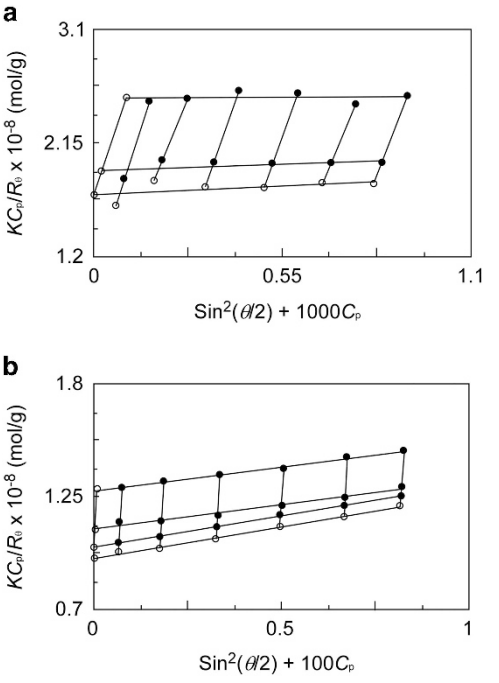

Figure 4 Zimm plots for (**a**) $PMPC_{82}$-*b*-$PChM_3$ and (**b**) $PMPC_{82}$-*b*-$PChM_6$ in water.

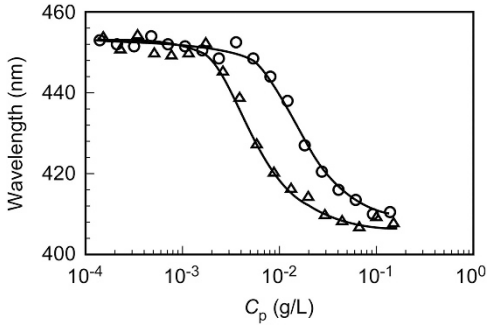

Figure 6 PNA fluorescence emission maxima as a function of the polymer concentration (C_p) for $PMPC_{82}$-*b*-$PChM_3$ (○) and $PMPC_{82}$-*b*-$PChM_6$ (Δ) in aqueous solutions.

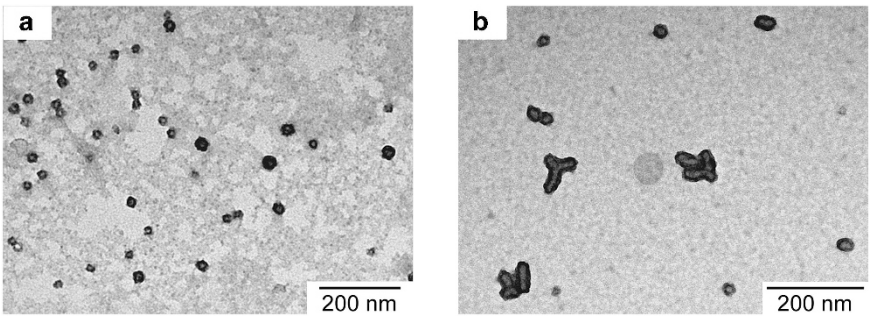

Figure 5 TEM images of (**a**) $PMPC_{82}$-*b*-$PChM_3$ and (**b**) $PMPC_{82}$-*b*-$PChM_6$ in water.

plotted as a function of C_p. The C_p value at which the maximum wavelength of PNA starts to blue shift was defined as CAC. The CAC values for $PMPC_{82}$-*b*-$PChM_3$ and $PMPC_{82}$-*b*-$PChM_6$ were observed to be 5.38×10^{-3} and 1.73×10^{-3} g l^{-1}, respectively. That is to say the CAC value decreases when the hydrophobic Chol content in the diblock copolymer increases.

CONCLUSION

$PMPC_{82}$-*b*-$PChM_n$ with a well-controlled structure was prepared via reversible addition–fragmentation chain transfer controlled/living radical polymerization using $PMPC_{82}$ macro-CTA. To obtain aqueous solutions of $PMPC_{82}$-*b*-$PChM_n$, the $PMPC_{82}$-*b*-$PChM_n$ was first dissolved in organic solvent and then dialyzed against pure water. The spherical micelles were formed from $PMPC_{82}$-*b*-$PChM_3$ in water and a morphology of mixtures of spherical and rod-like micelles was formed from $PMPC_{82}$-*b*-$PChM_6$ in water, as evidenced by the TEM observation results. The molecular weight ratio between hydrophilic PMPC and hydrophobic PChM is the dominant factor affecting the shape of the aggregates in water. When the Chol content in the polymer was increased, the shape of the aggregates changed from spherical to rod like. From the fluorescence probe study, it was observed that the aggregates formed from the diblock copolymer could incorporate hydrophobic small guest molecules into the hydrophobic domain, PChM blocks. The aggregates possessed a well-defined core-shell shape surrounded with biocompatible and hydrophilic PMPC shells. Therefore, it is expected that the aggregates studied can be a promising candidate for biocompatible drug delivery systems.

ACKNOWLEDGEMENTS

This work was financially supported by a Grant-in-Aid for Scientific Research (25288101) from the Japan Society for the Promotion of Science (JSPS) and the Network Joint Research Center for Materials and Devices (2013B25).

1 Abe, K., Koide, M. & Tsuchida, E. Selective complexation of macromolecules. *Macromolecules* **10**, 1259–1264 (1977).
2 Nakai, K., Nishiuchi, M., Inoue, M., Ishihara, K., Sanada, Y., Sakurai, K. & Yusa, S. Preparation and characterization of polyion complex micelles with phosphobetaine shells. *Langmuir* **29**, 9651–9661 (2013).
3 Zhang, L. & Eisenberg, A. Multiple morphologies and characteristics of "crew-cut" micelle-like aggregates of polystyrene-*b*-poly(acrylic acid) diblock copolymers in aqueous solutions. *J. Am. Chem. Soc.* **118**, 3168–3181 (1996).
4 Hayward, R. C. & Pochan, D. J. Tailored assemblies of block copolymers in solution: it is all about the process. *Macromolecules* **43**, 3577–3584 (2010).
5 Blanazs, A., Ryan, A. J. & Armes, S. P. Predictive phase diagrams for RAFT aqueous dispersion polymerization: effect of block copolymer composition, molecular weight, and copolymer concentration. *Macromolecules* **45**, 5099–5107 (2012).
6 Yamaguchi, T., Asada, T., Hayashi, H. & Nakamura, N. Dependence of the packing structure of mesogenic groups on the flexible spacer length of liquid crystalline side-chain polymers. *Macromolecules* **22**, 1141–1144 (1989).
7 Piñol, R., Jia, L., Gubellini, F., Lévy, D., Albouy, P. A., Keller, P., Cao, A. & Li, M. H. Self-assembly of PEG-*b*-liquid crystal polymer: the role of smectic order in the formation of nanofibers. *Macromolecules* **40**, 5625–5627 (2007).
8 Yang, H., Jia, L., Zhu, C., Di-Cicco, A., Levy, D., Albouy, P. A., Li, M. H. & Keller, P. Amphiphilic poly(ethylene oxide)-*block*-poly(butadiene-graft-liquid crystal) copolymers: Synthesis and self-assembly in water. *Macromolecules* **43**, 10442–10451 (2010).
9 Zhou, Y., Ahn, S. K., Lakhman, R. K., Gopinadhan, M., Osuji, C. O. & Kasi, R. M. Tailoring crystallization behavior of PEO-based liquid crystalline block copolymers through variation in liquid crystalline content. *Macromolecules* **44**, 3924–3934 (2011).
10 Boissé, S., Rieger, J., Di-Cicco, A., Albouy, P. A., Bui, C., Li, M. H. & Charleux, B. Synthesis via RAFT of amphiphilic block copolymers with liquid-crystalline hydrophobic block and their self-assembly in water. *Macromolecules* **42**, 8688–8696 (2009).
11 Jia, L., Cao, A., Levy, D., Xu, B., Albouy, P. A., Xing, X., Bowick, M. J. & Li, M. H. Smectic polymer vesicles. *Soft Matter* **5**, 3446–3451 (2009).
12 Venkataraman, S., Lee, A. L., Maune, H. T., Hedrick, J. L., Prabhu, V. M. & Yang, Y. Y. Formation of disk- and stacked-disk-like self-assembled morphologies from cholesterol-functionalized amphiphilic polycarbonate diblock copolymers. *Macromolecules* **46**, 4839–4846 (2013).
13 Ishihara, K., Ueda, T. & Nakabayasi, N. Cell membrane-inspired phospholipid polymers for developing medical devices with excellent biointerfaces. *Polym. J.* **22**, 355–360 (1990).
14 Lobb, E. J., Ma, I., Billingham, N. C., Armes, S. P. & Lewis, A. L. Facile synthesis of well-defined, biocompatible phosphorylcholine-based methacrylate copolymers via atom transfer radical polymerization at 20 °C. *J. Am. Chem. Soc.* **123**, 7913–7914 (2001).
15 Ma, I., Lobb, E. J., Billingham, N. C., Armes, S. P., Lewis, A. L., Lloyd, A. M. & Salvage, J. P. Synthesis of biocompatible polymers. 1. Homopolymerization of 2-methacryloyloxyethyl phosphorylcholine via ATRP in protic solvents: an optimization study. *Macromolecules* **35**, 9306–9314 (2003).
16 Iwasaki, Y. & Akiyoshi, K. Synthesis and characterization of amphiphilic polyphosphates with hydrophilic graft chains and cholesteryl groups as nanocarriers. *Biomacromolecules* **7**, 1433–1438 (2006).
17 Xu, J. P., Ji, J., Chen, W. D. & Shen, J. C. Novel biomimetic polymersomes as polymer therapeutics for drug delivery. *J. Control. Release* **107**, 502–512 (2005).
18 Shannon, P. J. Synthesis of methacrylate and acrylate monomers of cholesteric esters via phase-transfer catalysis. *Macromolecules* **16**, 1677–1678 (1983).
19 Mitsukami, Y., Donovan, M. S., Lowe, A. B. & McCormick, C. L. Water-soluble polymers. 81. Direct synthesis of hydrophilic styrenic-based homopolymers and block copolymers in aqueous solution via RAFT. *Macromolecules* **34**, 2248–2256 (2001).
20 Zimm, B. H. The scattering of light and radial distribution of high polymer solutions. *J. Chem. Phys.* **16**, 1093–1099 (1948).
21 Jakes, J. Regularized positive exponential sum (REPES) program-a way of investing Laplace transform data obtained by dynamic light scattering. *Collect. Czech. Chem. Commun.* **60**, 1781–1797 (1995).
22 Xu, R., Winnik, M. A., Hallett, F. R., Riess, G. & Crocher, M. D. Light-scattering study of the association behavior of styrene-ethylene oxide block copolymers in aqueous solution. *Macromolecules* **24**, 87–93 (1991).
23 Lima, M. M. D. S., Wong, J. T., Paillet, M., Borsali, R. & Pecora, R. Translational and rotational dynamics of rodlike cellulose whiskers. *Langmuir* **19**, 24–29 (2003).
24 Quintana, J. R., Jánez, M. D., Villacampa, M. & Katime, I. Diblock copolymer micelles in solvent binary mixtures. 1. Selective solvent precipitant. *Macromolecules* **28**, 4139–4143 (1995).
25 Villacampa, M., Apodaca, E. D., Quintana, J. R. & Katime, I. Diblock copolymer micelles in solvent binary mixtures. 2. Selective solvent/good solvent. *Macromolecules* **28**, 4144–4149 (1995).
26 Huber, K., Bantle, S., Lutz, P. & Burchard, W. Hydrodynamic and thermodynamic behavior of short-chain polystyrene in toluene and cyclohexane at 34.5 °C. *Macromolecules* **18**, 1461–1467 (1985).
27 Akcasu, A. Z. & Han, C. C. Molecular weight and temperature dependence of polymer dimensions in solution. *Macromolecules* **12**, 276–280 (1979).
28 Konishi, T., Yoshizaki, T. & Yamakawa, H. On the "universal constants" ρ and Φ of flexible polymers. *Macromolecules* **24**, 5614–5622 (1991).
29 He, W. D., Sun, X. L., Wan, W. M. & Pan, C. Y. Multiple morphologies of PAA-*b*-PSt assemblies throughout RAFT dispersion polymerization of styrene with PAA macro-CTA. *Macromolecules* **44**, 3358–3365 (2011).
30 McClure, W. O. & Wdelman, G. M. Fluorescent probes for conformational states of proteins. I. Mechanism of fluorescence of 2-*p*-toluidinylnaphthalene-6-sulfonate, a hydrophobic probe. *Biochemistry* **5**, 1908–1919 (1966).
31 Overath, P. & Träuble, H. Phase transitions in cells, membranes, and lipids of *Escherichia coli*. Detection by fluorescent probes, light scattering, and dilatometry. *Biochemistry* **12**, 2625–2634 (1973).